Supporting Information

High-rate capability of supercapacitors based on tannin-derived ordered mesoporous carbons

Jimena Castro-Gutiérrez,[†] *Noel Díez,*[‡] *Marta Sevilla,*[‡] *Maria Teresa Izquierdo,*[§] *Jaafar Ghanbaja,*[ǂ] *Alain Celzard,*[†] *and Vanessa Fierro*[†]*

[†] Université de Lorraine, Institut Jean Lamour, UMR CNRS 7198. 27 Rue Philippe Séguin, 88051 Epinal Cedex 9, France.

[‡] Instituto Nacional del Carbón (CSIC). P.O. Box 73, 33080 Oviedo, Spain

[§] Instituto de Carboquímica (ICB-CSIC). Miguel Luesma Castán 4, E-50018 Zaragoza, Spain

[ǂ] Université de Lorraine, Institut Jean Lamour UMR CNRS 7198. 2 Allée André Guinier, BP 50840, 54011 Nancy Cedex

Table S1. Pore texture parameters, calculated from N_2 and CO_2 adsorption isotherms, for the as-synthesised material and for the AOMCs.

Sample	Act. time [min]	BO	S_{NLDFT} [m^2g^{-1}]	A_{BET} [m^2g^{-1}]	V_{tot} [cm^3g^{-1}]	$V_{u\mu}$ [cm^3g^{-1}]	$V_{s\mu}$ [cm^3g^{-1}]	V_{meso} [cm^3g^{-1}]	w_{av} [nm]
CTPW	0	0	761	567	0.36	0.16	0.04	0.16	0.9
A15-CTPW	15	0.14	1085	894	0.54	0.21	0.10	0.23	1.0
A30-CTPW	30	0.32	1333	1222	0.71	0.22	0.20	0.29	1.1
A45-CTPW	45	0.41	1416	1387	0.80	0.22	0.26	0.33	1.1
A60-CTPW	60	0.43	1480	1479	0.86	0.20	0.30	0.35	1.2
A75-CTPW	75	0.59	1614	1867	1.11	0.14	0.48	0.49	1.4
A90-CTPW	90	0.78	1576	1999	1.23	0.09	0.54	0.60	1.6
A105-CTPW	105	0.75	1644	2061	1.19	0.12	0.55	0.53	1.5
A120-CTPW	120	0.94	1215	1642	0.95	0.06	0.42	0.47	1.6

BO: burn-off due to the activation process. S_{NLDFT} and A_{BET}: specific surface areas calculated by applying 2D-NLDFT HS and BET models, respectively. Parameters calculated from the 2D-NLDFT HS pore size distribution: V_{tot}, total pore volume; $V_{u\mu}$, ultramicropore volume (w < 0.7 nm); $V_{s\mu}$, supermicropore volume (0.7 < w < 2 nm); $V_{meso} = V_{tot} - V_{s\mu} - V_{u\mu}$, mesopore volume; w_{av}, average pore size.

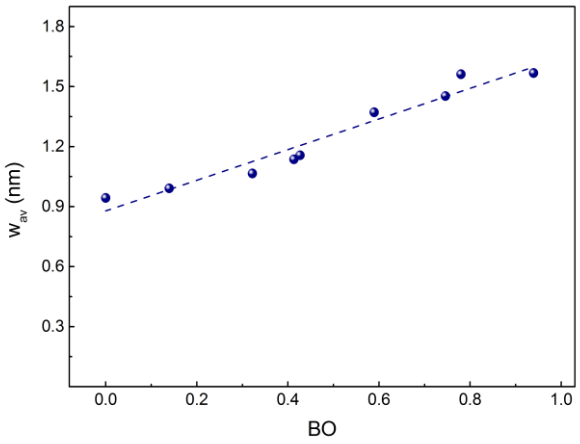

Figure S1. Average pore size as a function of burn-off (BO), calculated from the pore size distribution obtained by applying the 2D-NLDFT HS model to both N_2 and CO_2 isotherms. The straight line is just a guide for the eye.

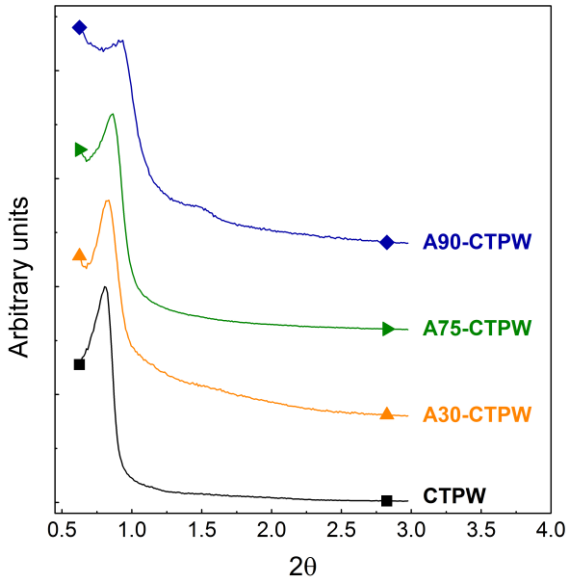

Figure S2. SAXS measurements for the as-synthesised material and for AOMCs activated during 30, 75 and 90 min.

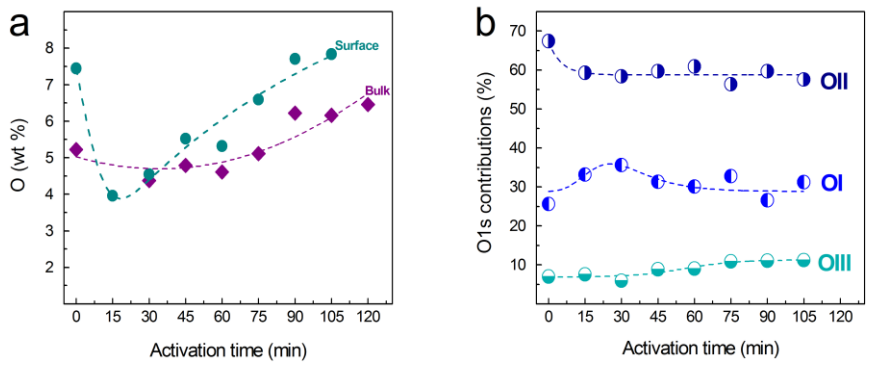

Figure S3. (a) Oxygen content measured in the bulk, by elemental analysis, and at the surface, measured by XPS. (b) Relative contributions to the oxygen surface functionalities. The dotted lines are only guides for the eye.

Table S2. Peak assignment and relative contributions of surface functionalities obtained by XPS analysis.

Sample	C1s contributions					O1s contributions			
	CI	CII	CIII	CIV	CV	OI	OII	OIII	O*
	A (BE) [% (eV)]	A (BE) [% (eV)]	A (BE) [% (eV)]	A (BE) [% (eV)]	A (BE) [% (eV)]	A (BE) [% (eV)]	A (BE) [% (eV)]	A (BE) [% (eV)]	A (BE) [% (eV)]
CTPW	68.3 (284.4)	26.9 (285.5)	3.6 (287.6)	1.2 (289.2)	--	25.6 (531.3)	67.4 (532.7)	7.0 (534.5)	
A30-CTPW	76.3 (284.5)	21.8 (285.5)	1.9 (287.6)	--	--	35.6 (531.1)	58.4 (532.8)	5.9 (534.5)	
A45-CTPW	75.1 (284.5)	22.9 (285.5)	2.0 (287.6)	--	--	31.3 (531.1)	59.7 (532.7)	8.9 (534.5)	
A60-CTPW	75.7 (284.5)	22.2 (285.5)	2.1 (287.6)	--	--	30.1 (531.1)	60.9 (532.7)	9.0 (534.5)	
A75-CTPW	74.6 (284.5)	23.5 (285.5)	1.9 (287.6)	--	--	32.8 (531.1)	56.4 (532.7)	10.9 (534.5)	
A90-CTPW	73.9 (284.5)	24.7 (285.5)	1.4 (287.6)	--	--	26.6 (531.2)	59.7 (532.6)	11.1 (534.5)	2.6 (536.2)
A105-CTPW	71.5 (284.5)	25.1 (285.5)	2.1 (287.6)	1.4 (289.2)	--	31.2 (531.4)	57.6 (532.8)	11.2 (534.9)	

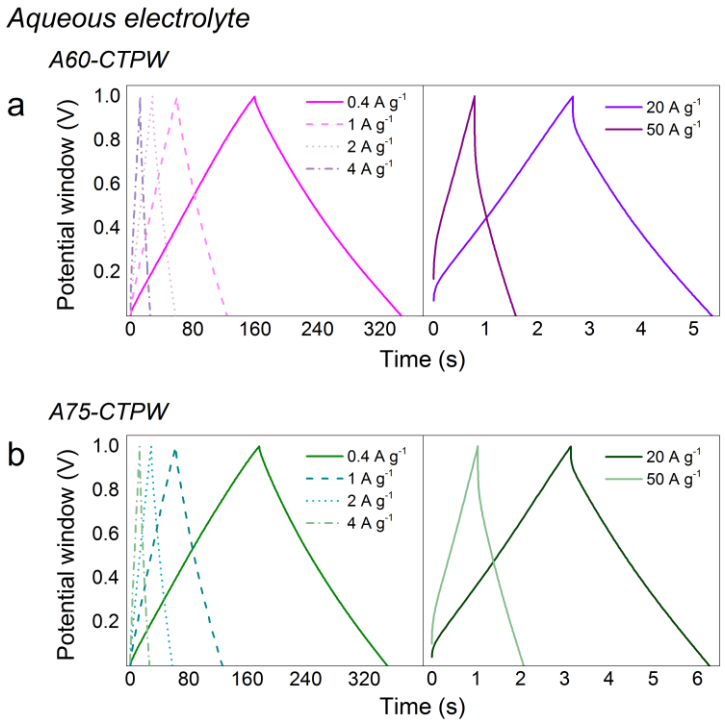

Figure S4. Charge-discharge curves for (a) A60-CTPW and (b) A75-CTPW in aqueous electrolyte.

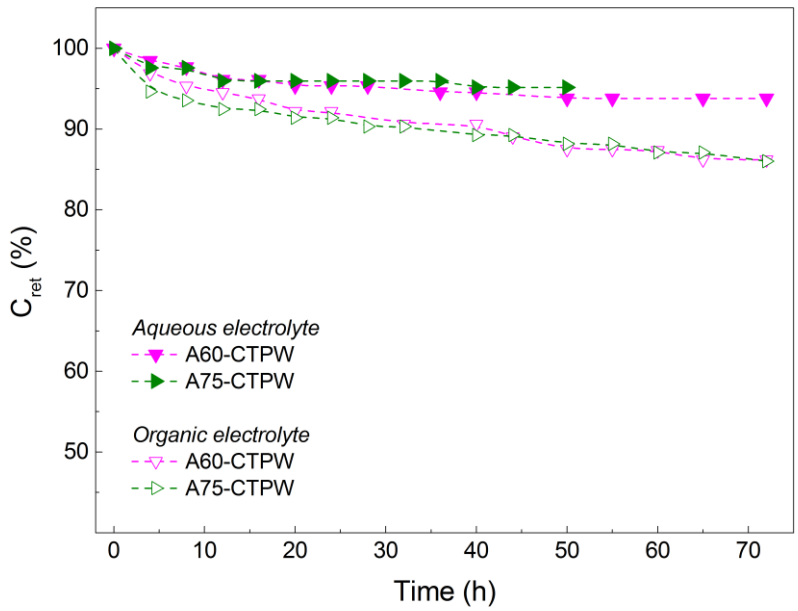

Figure S5. Capacitance retention over time by potentiostatic hold at maximum cell voltage in aqueous (1 V, solid symbols) and organic (2.7 V, open symbols) electrolytes.

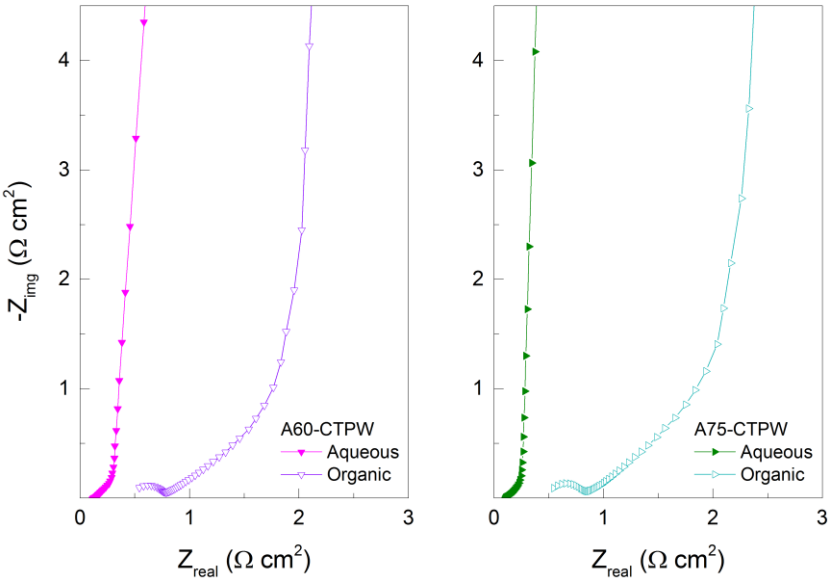

Figure S6. Nyquist plots for A60- and A75-CTPW in both aqueous and organic electrolytes.

Table S3. Single-electrode specific capacitance ($C_e = 4\,C_{cell}$) at 5 A g^{-1} of A60-CTPW and A75-CTPW and other non-doped materials with similar properties reported in the literature. The samples names correspond to their respective bibliographic references.[1–12]

Aqueous electrolyte (H_2SO_4)					Organic electrolyte ($TEABF_4$)				
Sample	**Cell type**	**Electrolyte concentration**	**Potential window**	**C_e**	**Sample**	**Cell type**	**Electrolyte concentration /Solvent**	**Potential window**	**Cell specific capacitance**
A60-CTPW A75-CTPW	2 electrodes	1 M	1 V	112 F g^{-1} 128 F g^{-1}	A60-CTPW A75-CTPW	2 electrodes	1 M / ACN	2.7 V	92 F g^{-1} 92 F g^{-1}
C3/30	2 electrodes	2 M	0.8 V	140 F g^{-1}	SWNT solid	2 electrodes	1 M / PC	2.5 V	44 F g^{-1}
AOW	2 electrodes	1 M	1 V	120 F g^{-1}	Aerosol-carbon	3 electrodes	1 M / PC	2.7 V	96 F g^{-1}
MC-1	3 electrodes	2 M	0.7 V	172 F g^{-1}	MC-1	3 electrodes	1 M / PC	3 V	80 F g^{-1}
C-1* C-2*	2 electrodes	1 M	1 V	144 F g^{-1} 132 F g^{-1}	C-1* C-2*	2 electrodes	1 M / ACN	2 V	88 F g^{-1} 80 F g^{-1}
PhC GaC CatC TanC	2 electrodes	1 M	0.8 V	148 F g^{-1} 128 F g^{-1} 128 F g^{-1} 116 F g^{-1}	CGC-3.5 CGC-5	2 electrodes	1 M / ACN	2.7 V	80 F g^{-1} 120 F g^{-1}
L-b-700 L-b-900 L-Y-700 L-Y-900	3 electrodes	1 M	0.8 V	76 F g^{-1} 80 F g^{-1} 52 F g^{-1} 124 F g^{-1}	NPV1 NPV2	2 electrodes	1 M / PC	2.5 V	52 F g^{-1} 80 F g^{-1}
AC-KOH	3 electrodes	1 M	1 V	132 F g^{-1}					
ACM-B	2 electrodes	1 M	1 V	100 F g^{-1}					

* Measured at 1 A g^{-1}, the maximum reported in the corresponding study. ACN and PC stand for acetonitrile and propylene carbonate, respectively.

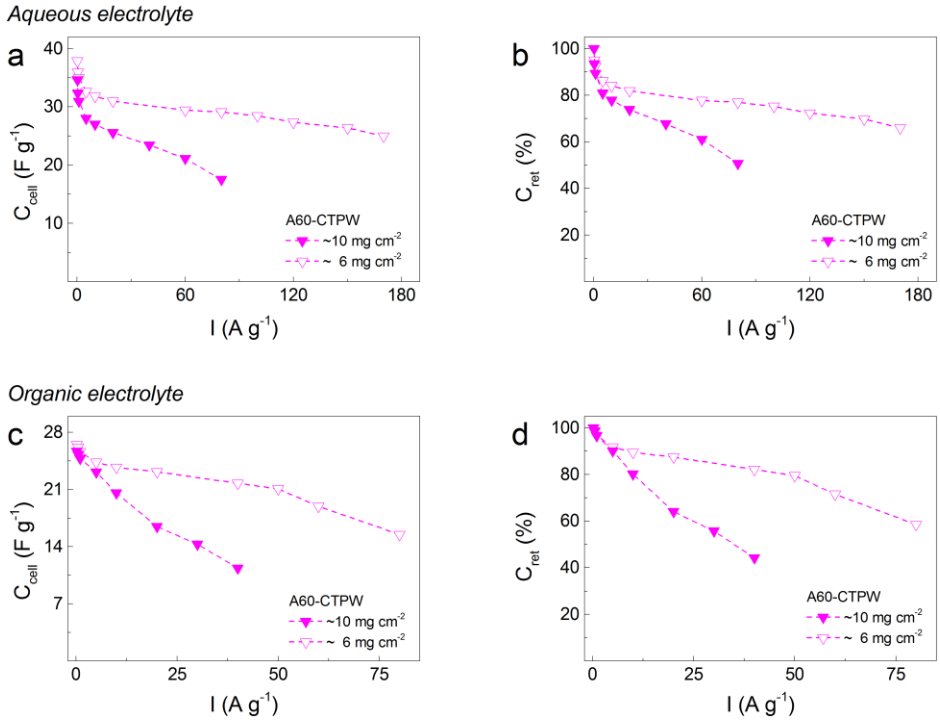

Figure S7. Cell specific capacitance, C_{cell}, and capacitance retention, C_{ret}, of A60-CTPW in (a,b) aqueous and (c,d) organic electrolytes, calculated from GCD tests at different current densities using electrodes with carbon loads of ~10 and ~6 mg cm^{-2}.

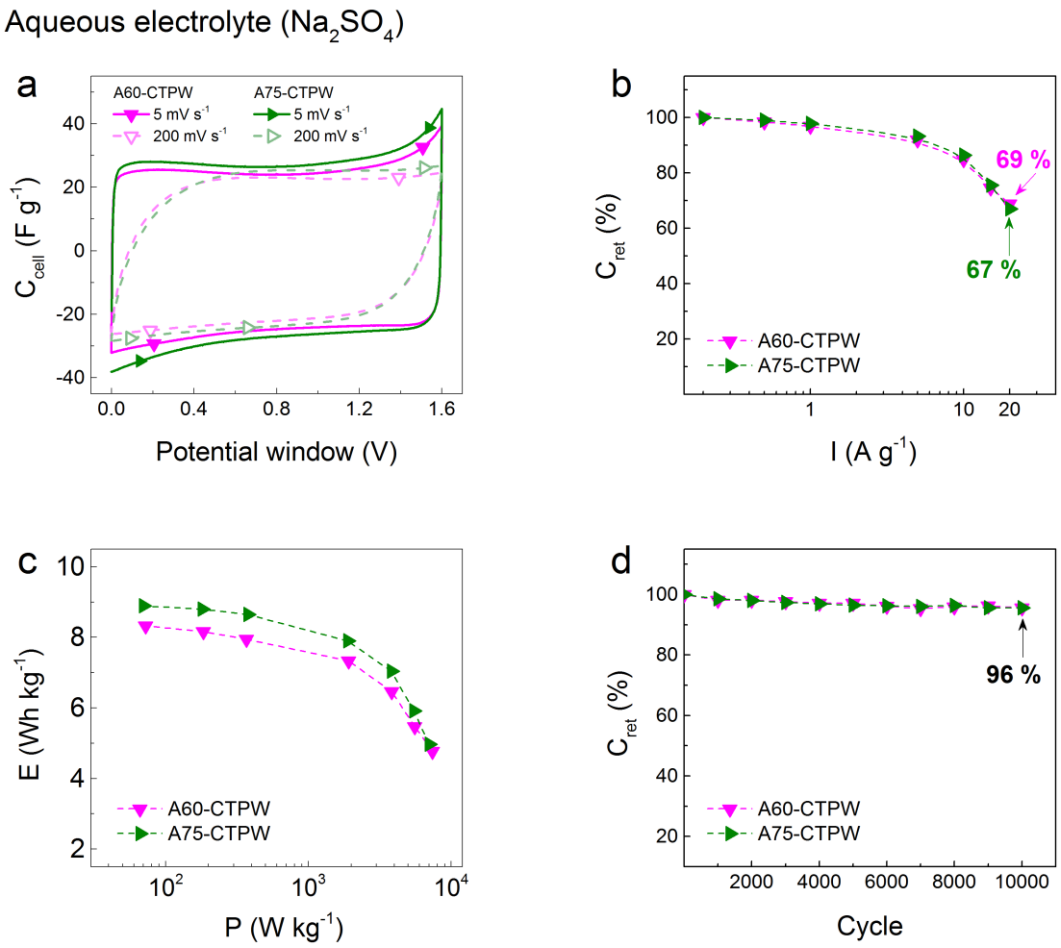

Figure S8. Electrochemical performance of A60-CTPW and A75-CTPW in $NaSO_4$ as aqueous electrolyte: (a) CV curves at 5 and 200 mV s^{-1}; (b) capacitance retention versus applied current ; (c) Ragone-like plot for the achieved specific energy and power of the assembled SCs; (d) capacitance retention after continuous cycling at 5 A g^{-1}. The potential window was 1.6 V in all cases.

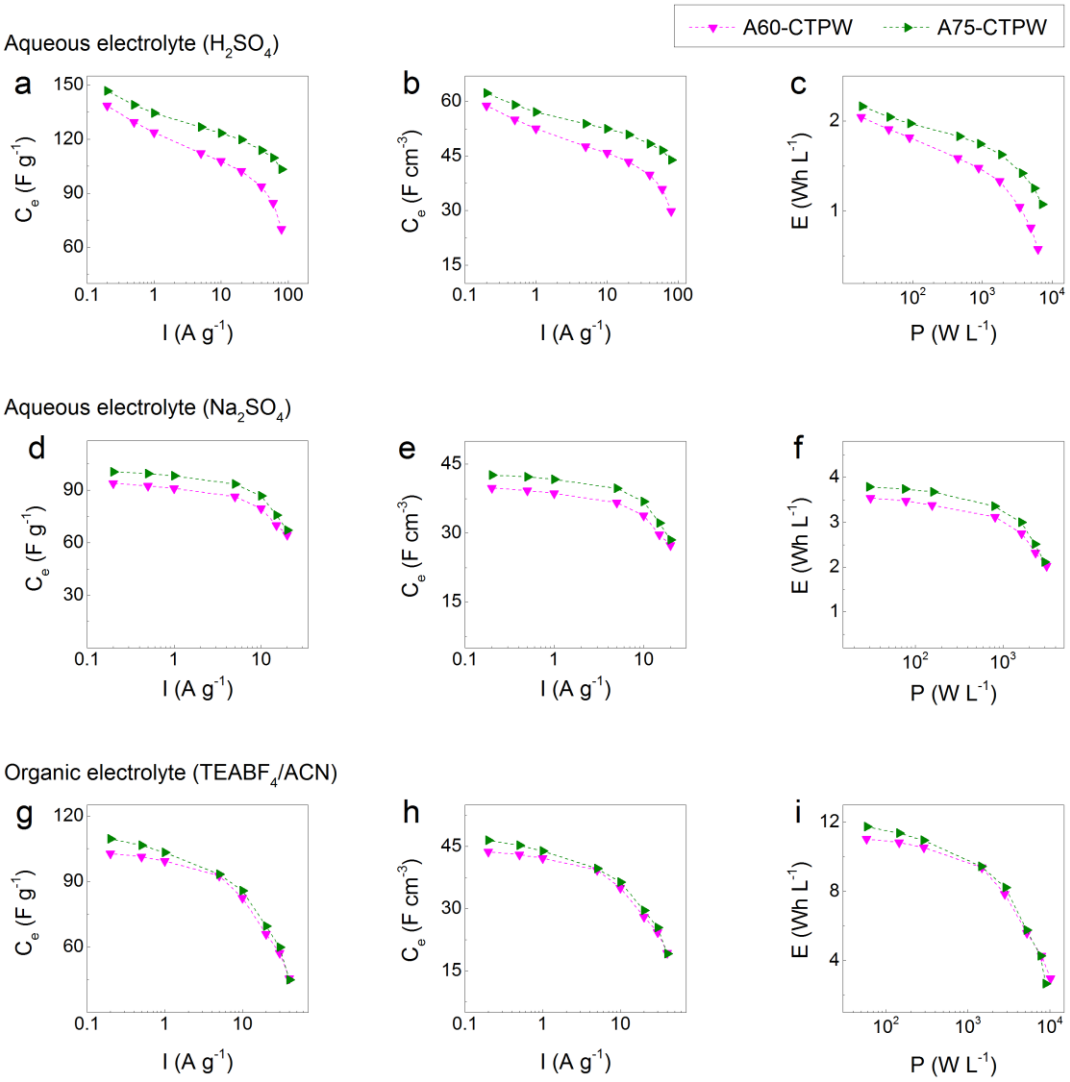

Figure S9. (a, d, g) Gravimetric and (b, e, h) volumetric single-electrode capacitance as a function of the applied current, and (c, f, i) Ragone-like plot presenting the achieved specific energy and power. Values presented for both tested materials, A60-CTPW and A75-CTPW, in the three electrolytes: (a, b, c) 1 M H_2SO_4, (d, e, f) 1 M Na_2SO_4 and (g, h, i) 1 M $TEABF_4$/ACN.

References

(1) Sanchez-Sanchez, A.; Izquierdo, M. T.; Medjahdi, G.; Ghanbaja, J.; Celzard, A.; Fierro, V. Ordered Mesoporous Carbons Obtained by Soft-Templating of Tannin in Mild Conditions. *Microporous and Mesoporous Materials* **2018**, *270*, 127–139. https://doi.org/10.1016/j.micromeso.2018.05.017.

(2) Elmouwahidi, A.; Castelo-Quibén, J.; Vivo-Vilches, J. F.; Pérez-Cadenas, A. F.; Maldonado-Hódar, F. J.; Carrasco-Marín, F. Activated Carbons from Agricultural Waste Solvothermally Doped with Sulphur as Electrodes for Supercapacitors. *Chemical Engineering Journal* **2018**, *334*, 1835–1841. https://doi.org/10.1016/j.cej.2017.11.141.

(3) Sanchez-Sanchez, A.; Izquierdo, M. T.; Ghanbaja, J.; Medjahdi, G.; Mathieu, S.; Celzard, A.; Fierro, V. Excellent Electrochemical Performances of Nanocast Ordered Mesoporous Carbons Based on Tannin-Related Polyphenols as Supercapacitor Electrodes. *Journal of Power Sources* **2017**, *344*, 15–24. https://doi.org/10.1016/j.jpowsour.2017.01.099.

(4) Li, Z.; Zhang, L.; Amirkhiz, B. S.; Tan, X.; Xu, Z.; Wang, H.; Olsen, B. C.; Holt, C. M. B.; Mitlin, D. Carbonized Chicken Eggshell Membranes with 3D Architectures as High-Performance Electrode Materials for Supercapacitors. *Advanced Energy Materials* **2012**, *2* (4), 431–437. https://doi.org/10.1002/aenm.201100548.

(5) Ruiz, V.; Blanco, C.; Santamaría, R.; Ramos-Fernández, J. M.; Martínez-Escandell, M.; Sepúlveda-Escribano, A.; Rodríguez-Reinoso, F. An Activated Carbon Monolith as an Electrode Material for Supercapacitors. *Carbon* **2009**, *47* (1), 195–200. https://doi.org/10.1016/j.carbon.2008.09.048.

(6) Li, Q.; Jiang, R.; Dou, Y.; Wu, Z.; Huang, T.; Feng, D.; Yang, J.; Yu, A.; Zhao, D. Synthesis of Mesoporous Carbon Spheres with a Hierarchical Pore Structure for the Electrochemical Double-Layer Capacitor. *Carbon* **2011**, *49* (4), 1248–1257. https://doi.org/10.1016/j.carbon.2010.11.043.

(7) Fuertes, A. B.; Lota, G.; Centeno, T. A.; Frackowiak, E. Templated Mesoporous Carbons for Supercapacitor Application. *Electrochimica Acta* **2005**, *50* (14), 2799–2805. https://doi.org/10.1016/j.electacta.2004.11.027.

(8) Ruiz-Rosas, R.; Valero-Romero, M. J.; Salinas-Torres, D.; Rodríguez-Mirasol, J.; Cordero, T.; Morallón, E.; Cazorla-Amorós, D. Electrochemical Performance of Hierarchical Porous Carbon Materials Obtained from the Infiltration of Lignin into Zeolite Templates. *ChemSusChem* **2014**, *7* (5), 1458–1467. https://doi.org/10.1002/cssc.201301408.

(9) Futaba, D. N.; Hata, K.; Yamada, T.; Hiraoka, T.; Hayamizu, Y.; Kakudate, Y.; Tanaike, O.; Hatori, H.; Yumura, M.; Iijima, S. Shape-Engineerable and Highly Densely Packed Single-Walled Carbon Nanotubes and Their Application as Super-Capacitor Electrodes. *Nature Materials* **2006**, *5* (12), 987–994. https://doi.org/10.1038/nmat1782.

(10) Chen, Z.; Wen, J.; Yan, C.; Rice, L.; Sohn, H.; Shen, M.; Cai, M.; Dunn, B.; Lu, Y. High-Performance Supercapacitors Based on Hierarchically Porous Graphite Particles.

Advanced Energy Materials **2011**, *1* (4), 551–556. https://doi.org/10.1002/aenm.201100114.

(11) Xu, B.; Wu, F.; Mu, D.; Dai, L.; Cao, G.; Zhang, H.; Chen, S.; Yang, Y. Activated Carbon Prepared from PVDC by NaOH Activation as Electrode Materials for High Performance EDLCs with Non-Aqueous Electrolyte. *International Journal of Hydrogen Energy* **2010**, *35* (2), 632–637. https://doi.org/10.1016/j.ijhydene.2009.10.110.

(12) Rufford, T. E.; Hulicova-Jurcakova, D.; Fiset, E.; Zhu, Z.; Lu, G. Q. Double-Layer Capacitance of Waste Coffee Ground Activated Carbons in an Organic Electrolyte. *Electrochemistry Communications* **2009**, *11* (5), 974–977. https://doi.org/10.1016/j.elecom.2009.02.038.